1-14-2008

Polarization properties of retroreflecting right-angle prisms

R. M.A. Azzam
University of New Orleans, razzam@uno.edu

H. K. Khanfar

Recommended Citation

R. M. A. Azzam and H. K. Khanfar, "Polarization properties of retroreflecting right-angle prisms," Appl. Opt. 47, 359-364 (2008).

Polarization properties of retroreflecting right-angle prisms

R. M. A. Azzam* and H. K. Khanfar

Department of Electrical Engineering, University of New Orleans, New Orleans, Louisiana 70148, USA

*Corresponding author: razzam@uno.edu

Received 2 October 2007; accepted 3 November 2007;
posted 4 December 2007 (Doc. ID 88134); published 14 January 2008

The cumulative retardance Δ_t introduced between the p and the s orthogonal linear polarizations after two successive total internal reflections (TIRs) inside a right-angle prism at complementary angles ϕ and $90° - \phi$ is calculated as a function of ϕ and prism refractive index n. Quarter-wave retardation (QWR) is obtained on retroreflection with minimum angular sensitivity when $n = (\sqrt{2} + 1)^{1/2} = 1.55377$ and $\phi = 45°$. A QWR prism made of N-BAK4 Schott glass ($n = 1.55377$ at $\lambda = 1303.5$ nm) has good spectral response ($<5°$ retardance error) over the 0.5–2 μm visible and near-IR spectral range. A ZnS-coated right-angle Si prism achieves QWR with an error of $<\pm 2.5°$ in the 9–11 μm (CO_2 laser) IR spectral range. This device functions as a linear-to-circular polarization transformer and can be tuned to exact QWR at any desired wavelength (within a given range) by tilting the prism by a small angle around $\phi = 45°$. A PbTe right-angle prism introduces near-half-wave retardation (near-HWR) with a ≤2% error over a broad ($4 \leq \lambda \leq 12.5$ μm) IR spectral range. This device also has a wide field of view and its interesting polarization properties are discussed. A compact (aspect ratio of 2), in-line, HWR is described that uses a chevron dual Fresnel rhomb with four TIRs at the same angle $\phi = 45°$. Finally, a useful algorithm is presented that transforms a three-term Sellmeier dispersion relation of a transparent optical material to an equivalent cubic equation that can be solved for the wavelengths at which the refractive index assumes any desired value.

OCIS codes: 160.2750, 230.5440, 230.5480, 240.0240, 260.2130, 260.3060.

1. Introduction

Quarter- and half-wave retarders that use one or more total internal reflections (TIRs) in a Fresnel rhomb or prism have been studied extensively [1–9]. For versatility in polarization state generation and detection, it is desirable to have an in-line multiple-reflection device that can be rotated about the light-beam axis. However, for certain applications a fixed device is adequate for achieving a specific (e.g., linear-to-circular) polarization transformation in addition to a beam-steering function.

In this paper the conditions for obtaining quarter- and half-wave retardation (QWR and HWR, respectively) when a light beam is retroreflected by a transparent, optically isotropic, right-angle prism (Fig. 1) are considered. In Section 2 the cumulative differential phase shift (or retardance) Δ_t, introduced between the p and the s linear polarizations after two successive TIRs at angles of incidence ϕ and $90° - \phi$, is determined as a function of ϕ and for different values of the prism refractive index n. QWR is obtained with minimum angular sensitivity when $n = (\sqrt{2} + 1)^{1/2} = 1.55377$ at equal angles of 45°. In Section 3 several Schott glasses that have this refractive index are considered and good spectral response is demonstrated for a QWR prism made of N-BAK4 Schott glass over a broad (0.5 to 2 μm) spectral range in the visible and near IR.

In Section 4 a ZnS-coated right-angle Si prism is introduced that functions as an IR retroreflecting quarter-wave retarder in the 9–11 μm CO_2 laser spectral range. This device functions as a linear-to-circular polarization transformer and can be continuously tuned to exact QWR at any desired wavelength (within a given range) by rocking the

0003-6935/08/030359-06$15.00/0

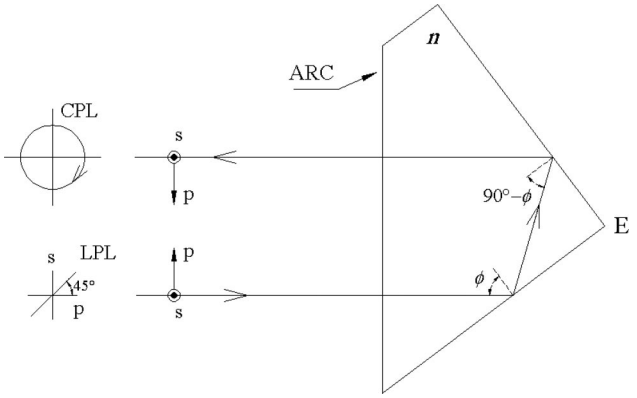

Fig. 1. Retroreflection of a monochromatic light beam via two successive TIRs at angles of incidence ϕ and $90° - \phi$ inside a prism of refractive index n. Light enters and leaves the prism normal to its entrance face, which is ARC. p and s are the linear polarizations parallel and perpendicular to the common plane of incidence, respectively (s is parallel to the edge of prism E). When the cumulative retardance is quarter-wave, incident linearly polarized light becomes circularly polarized upon retroreflection.

prism by a small angle. In Section 5 a PbTe right-angle prism is shown to perform as a near half-wave retarder (to within 2% retardance error) over a broad IR spectral range (4–12.5 μm) and a very wide field of view. The interesting polarization properties of retroreflection near-HWR are discussed. In Section 6 an angle-insensitive, in-line, HWR that uses four TIRs at the same angle ($\phi = 45°$) is described. Finally, Section 7 gives a brief summary of the paper. The retroreflecting QWR described in this paper has potential practical applications in return-path ellipsometers [10,11] and polarimetric refractometers [12].

2. Cumulative Differential Phase Shift on Retroreflection by a Right-Angle Prism

Figure 1 shows the retroreflection of a monochromatic light beam via two successive TIRs at angles of incidence ϕ and $90° - \phi$ inside a prism of refractive index n. Light enters and leaves the prism normal to its entrance face, which is antireflection coated (ARC). The cumulative TIR differential phase shift (retardance) Δ_t introduced after two TIRs in the prism is given by

$$\Delta_t(\phi) = \Delta(\phi) + \Delta(90° - \phi), \tag{1}$$

$$\Delta(\phi) = 2\tan^{-1}\left[\left(n^2\sin^2\phi - 1\right)^{1/2}/(n\sin\phi\tan\phi)\right], \tag{2}$$

[1,13]. For TIR the angle of incidence ϕ is limited to the range

$$\sin^{-1}(1/n) = \phi_c \le \phi \le 90° - \phi_c, \tag{3}$$

where ϕ_c is the critical angle. In the symmetric orientation of the prism with equal incidence angles, $\phi = 90° - \phi = 45°$, Eqs. (1) and (2) give

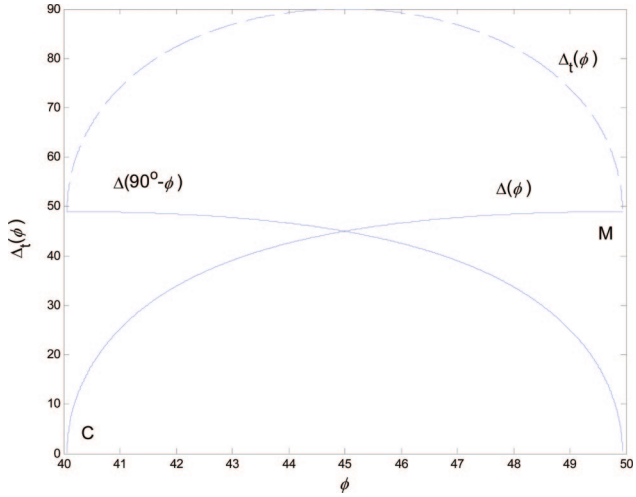

Fig. 2. (Color online) Plot of each of the three terms that appear in Eq. (1) as a function of ϕ in the range $\sin^{-1}(1/n) = \phi_c \le \phi \le 90° - \phi_c$, when $n = (\sqrt{2} + 1)^{1/2} = 1.55377$.

$$\Delta_t(45°) = 4\tan^{-1}\left[\left(n^2 - 2\right)^{1/2}/n\right]. \tag{4}$$

From Eq. (4) QWR, i.e.,

$$\Delta_t(45°) = \pi/2 \tag{5}$$

is obtained if

$$\left[\left(n^2 - 2\right)^{1/2}/n\right] = \tan(\pi/8) = \sqrt{2} - 1,$$
$$n = \left(\sqrt{2} + 1\right)^{1/2} = 1.55377. \tag{6}$$

Figure 2 is a plot of each of the three terms that appear in Eq. (1) as a function of ϕ in the range given by Eq. (3), when $n = (\sqrt{2} + 1)^{1/2} = 1.55377$. From Fig. 2 it is apparent that at $\phi = 45°$ we obtain

$$\Delta_t = 90°, \qquad \partial\Delta_t/\partial\phi = 0. \tag{7}$$

To prove the zero-derivative condition in Eq. (7), note that the function given by Eq. (1) is of the general form

$$g(x) = f(x) + f(a - x), \tag{8}$$

where a is a constant. By taking the first derivative of Eq. (8) with respect to x, one gets

$$g'(x) = f'(x) - f'(a - x). \tag{9}$$

Evaluation of Eq. (9) at $x = a/2$ yields

$$g'(a/2) = 0. \tag{10}$$

The same argument can be extended to prove that all higher-order odd-numbered derivatives of $g(x)$ at $x = a/2$ are also zero.

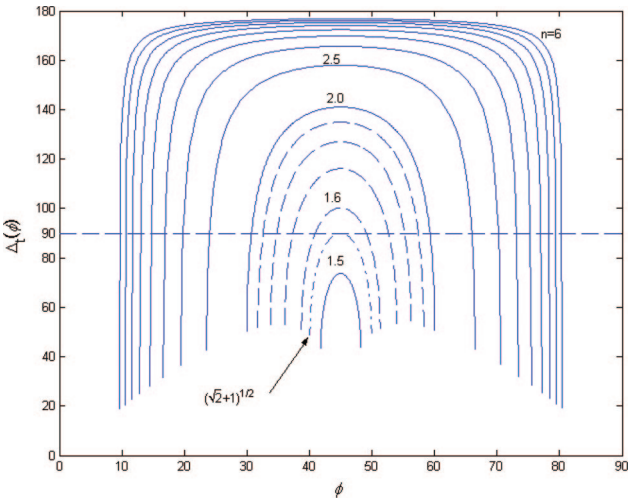

Fig. 3. (Color online) Cumulative retardance $\Delta_t(\phi)$ versus ϕ in the range $\phi_c \le \phi \le 90° - \phi_c$ for values of n from 1.5 to 6.0 in equal steps of 0.5 (solid curves) and from 1.6 to 1.9 in steps of 0.1 (dashed curves). The dashed–dotted curve corresponds to $n = (\sqrt{2} + 1)^{1/2}$.

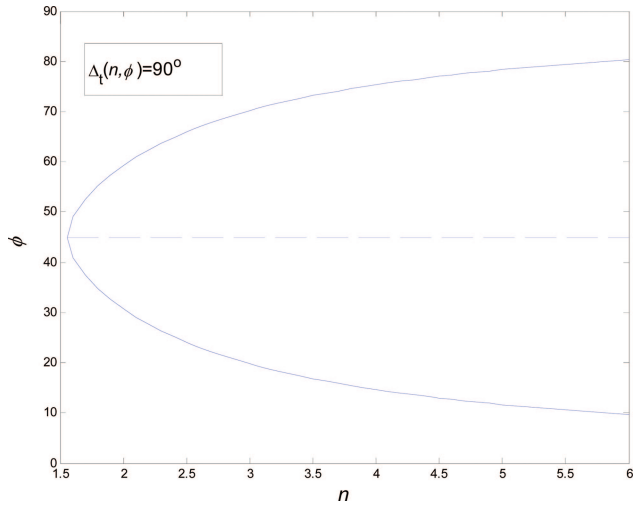

Fig. 4. (Color online) Locus of all possible combinations (n, ϕ) that produce QWR, $\Delta_t(n, \phi) = 90°$, on retroreflection by a right-angle prism.

In [13] $n = (\sqrt{2} + 1)^{1/2} = 1.55377$ is found to maximize the separation between the angle ϕ_m at which $\Delta(\phi)$ reaches its peak (point M in Fig. 2) and the critical angle ϕ_c (point C in Fig. 2). Also, when $n = (\sqrt{2} + 1)^{1/2}$, $\phi_m = 90° - \phi_c$, and the operating angle is $\phi = (\phi_m + \phi_c)/2 = 45°$. It is also interesting to note that the square of the refractive index given by Eq. (6) [i.e., $n = (\sqrt{2} + 1) = 2.41421$] is the minimum refractive index required for obtaining QWR on single TIR [9].

Figure 3 is a plot of $\Delta_t(\phi)$ versus ϕ in the range $\phi_c \le \phi \le 90° - \phi_c$ for values of n from 1.5 to 6.0 in equal steps of 0.5 (solid curves) and from 1.6 to 1.9 in steps of 0.1 (dashed curves). The dashed–dotted curve in Fig. 3 corresponds to $n = (\sqrt{2} + 1)^{1/2}$ and touches the line $\Delta_t(\phi) = 90°$ at $\phi = 45°$. Figure 3 also indicates that QWR [$\Delta_t(\phi) = 90°$] is achieved in retroreflection by a right-angle prism at unequal angles $(\phi, 90° - \phi)$ for any $n > 1.55377$; however, the angular sensitivity deteriorates rapidly as n increases. Figure 4 represents the constraint on (n, ϕ) such that $\Delta_t(n, \phi) = 90°$ on retroreflection.

3. Schott-Glass Right-Angle Prisms as Retroreflecting Quarter-Wave Retarders

Figure 5 shows a family of curves of $n(\lambda)$ versus wavelength λ of four Schott glasses with dispersion formulas [14] of the form

$$n^2 - 1 = \frac{B_1\lambda^2}{\lambda^2 - C_1} + \frac{B_2\lambda^2}{\lambda^2 - C_2} + \frac{B_3\lambda^2}{\lambda^2 - C_3}. \qquad (11)$$

All the curves in Fig. 5 intersect the line $n = (\sqrt{2} + 1)^{1/2} = 1.55377$. Table 1 identifies the four Schott glasses and lists the constants (B_j, C_j), $j = 1, 2, 3$ of their dispersion relations as well as the calculated wavelengths in nanometers at which $n = 1.55377$. The wavelengths at which the refractive index n, given by Eq. (11), assumes any specific value are readily obtained by solving a cubic equation in λ^2. The coefficients of the equivalent cubic equation are given in Appendix A for reference.

From Fig. 5 it is apparent that, of the four selected Schott glasses, N-BAK4 is best-suited for the current application. Figure 6 shows $n(\lambda)$ and $\Delta_t(\lambda)$ versus wavelength λ for an uncoated N-BAK4 right-angle prism (in the symmetric $\phi = 45°$ orientation) over the $0.5 \le \lambda \le 2$ μm spectral range. The maximum deviation from QWR, over two octaves in the visible and near-IR spectrum, is $<5°$, which is impressive. The retardance error of the device within the light wave communications wave band $1.3 \le \lambda \le 1.6$ μm is $<2°$.

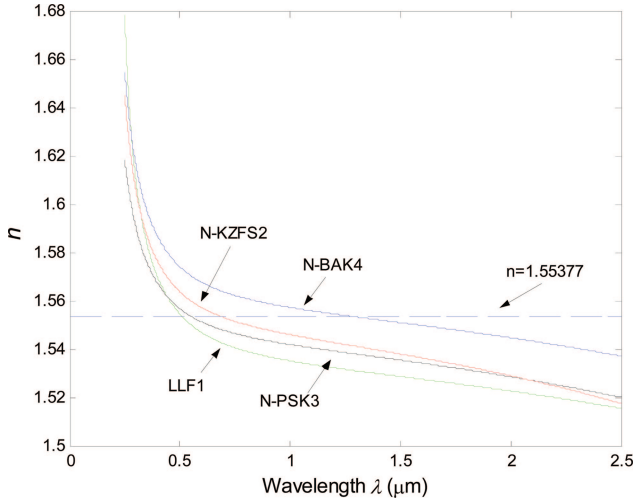

Fig. 5. (Color online) Refractive index $n(\lambda)$ plotted versus wavelength λ for four different Schott glasses with dispersion formulas given by Eq. (11) and Table 1. All the curves intersect the line $n = (\sqrt{2} + 1)^{1/2} = 1.55377$ at wavelengths that are listed in the last row of Table 1.

Table 1. Constants [(B_i, C_i), i = 1, 2, 3] of the Dispersion Formulas [Eq. (11)] of Four Schott Optical Glasses and the Wavelengths λ at Which the Refractive Index n = 1.55377

	Glass Type			
	LLF1	N-PSK3	N-KZFS2	N-BAK4
B_1	1.21640125	0.88727211	1.23697554	1.28834642
B_2	0.13366454	0.489592425	0.153569376	0.132817724
B_3	0.883399468	1.04865296	0.903976272	0.945395373
C_1	0.00857807248	0.00469824067	0.00747170505	0.00779980626
C_2	0.0420143003	0.0161818463	0.0308053556	0.0315631177
C_3	107.59306	104.374975	70.1731084	105.965875
λ (nm)	513.22	557.67	694.64	1303.50

4. Infrared Quarter-Wave Retarder Using ZnS-Coated Right-Angle Si Prism

This quarter-wave retarder transforms the state of polarization of an IR (e.g., CO_2 laser) beam in the $9 \le \lambda \le 11$ μm spectral range from linear to circular, as shown in Fig. 7. The ZnS coating thickness is assumed to be much greater than the penetration depth of the evanescent field in TIR at the Si–ZnS interface, so that light interference in the film is nonexistent or negligible. The differential phase shift on TIR is determined by the relative refractive index

$$n = n(\mathrm{Si})/n(\mathrm{ZnS}). \tag{12}$$

From the published dispersion relations of Si and ZnS [15], $n(\lambda)$ of Eq. (12) and $\Delta_t(\lambda)$ are calculated and plotted in Fig. 8 as functions of λ in the $9 \le \lambda \le 11$ μm spectral range for the symmetric $\phi = 45°$ orientation of the prism (Fig. 7). The wavelength at which $n(\mathrm{Si})/n(\mathrm{ZnS}) = 1.55377$ and $\Delta_t(\lambda) = 90°$ is $\lambda = 10.039$ μm. Figure 8 shows that the retardance error is $<\pm 2.5°$ over the 2 μm bandwidth. The device is also angle insensitive because (1) $\partial\Delta_t/\partial\phi = 0$, and (2) light is strongly refracted toward the normal as it enters the prism at the air–Si interface.

Exact QWR [$\Delta_t(\lambda, \phi) = 90°$] can be maintained as the wavelength is changed by simply tilting the prism away from the symmetric position by a small angle. Figure 9 represents the constraint on λ and φ such that $\Delta_t(\lambda, \phi)$ assumes constant values from 88° to 92° in steps of 0.5°. The angle-of-incidence tunability is an important feature of this retarder. Polarization changes associated with wave refraction at small angles, as the light beam enters and leaves the hypotenuse face of the tilted prism, are negligible in the presence of the antireflection coating [16].

5. Polarization-Altering Properties of High-Index (PbTe) Retroreflecting Right-Angle Prism

A striking feature of Fig. 3 is that for large values of n the cumulative retardance $\Delta_t(\phi)$ is nearly flat with respect to incidence angle over a large range of φ around $\phi = 45°$. The maximum flat-top retardance $\Delta_{t\,\max}$ approaches 180° (HWR) asymptotically as $n \to \infty$. For $n = 6$, Eq. (4) gives $\Delta_{t\,\max} = 176.726°$, so that the retardance error (deviation from HWR) is only 3.274°. For $n \gg 1$, the retardance error RE in radians is approximately given by the simple formula

$$RE \approx \pi - (2/n^2), \tag{13}$$

as can be derived from Eq. (4).

An IR-transparent material with $n = 6$ is PbTe. Its refractive index [15] is given by a single-term Sellmeier dispersion relation of the form of Eq. (11) with $B_1 = 30.046$, $C_1 = (1.563)^2$, $B_2 = B_3 = 0$ in the $4 \le \lambda \le 12.5$ μm spectral range. The maximum

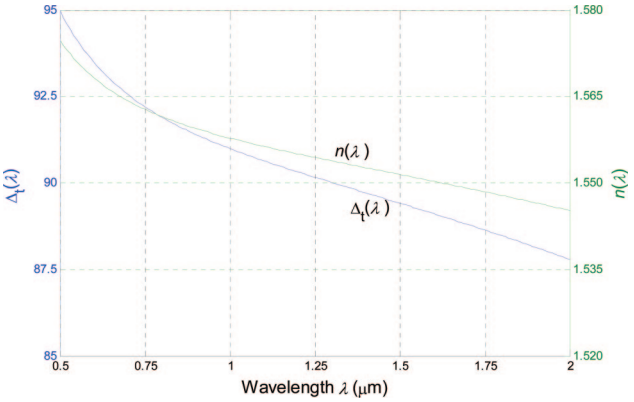

Fig. 6. (Color online) Refractive index $n(\lambda)$ and cumulative retardance $\Delta_t(\lambda)$ plotted versus wavelength λ for an uncoated N-BAK4 Schott glass right-angle prism in the symmetric $\phi = 45°$ orientation over the $0.5 \le \lambda \le 2$ μm spectral range.

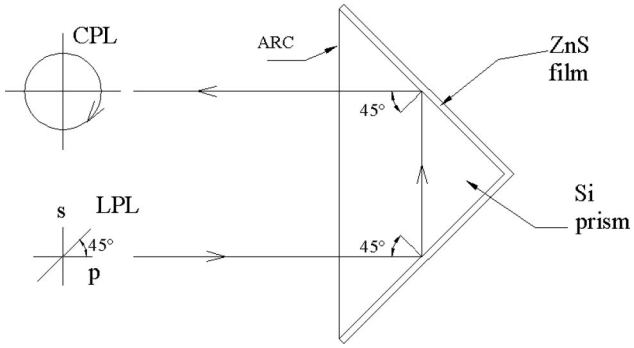

Fig. 7. ZnS-coated Si right-angle prism (in the symmetric orientation) transforms the state of polarization of an IR (e.g., CO_2 laser) beam from linear to circular. The entrance face of the prism is ARC.

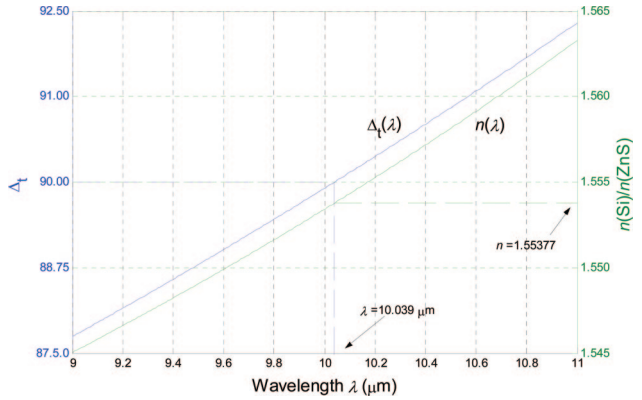

Fig. 8. (Color online) Relative refractive index $n(\lambda)$ [Eq. (12)] and cumulative retardance $\Delta_t(\lambda)$ of a ZnS-coated Si right-angle prism as functions of λ in the $9 \leq \lambda \leq 11$ μm spectral range for the symmetric ($\phi = 45°$) orientation of the prism, shown in Fig. 7. The relative refractive index $n(\mathrm{Si})/n(\mathrm{ZnS}) = 1.55377$ at wavelength $\lambda = 10.039$ μm.

$RE = 3.755°$ occurs at $\lambda = 12.5$ μm and $n = 5.6146$; over the entire transparency range of PbTe the deviation from HWR is <2.1%.

The combination of near-HWR and exact reversal of the direction of propagation upon retroreflection by a right-angle PbTe prism actually makes the device essentially polarization preserving for all incident states. For incident linearly polarized (LP) light at azimuth angle θ_i, the reflected polarization is slightly elliptical but is oriented at the same azimuth $\theta_r = \theta_i$ [Fig. 10(a)]. [The ellipticity of the reflected state is exaggerated in Fig. 10(a).] The small induced ellipticity e ($e = b/a$, the minor axis–major axis ratio of the reflected polarization ellipse) is related to the RE by

$$e = (RE/2)\sin 2\theta_i. \tag{14}$$

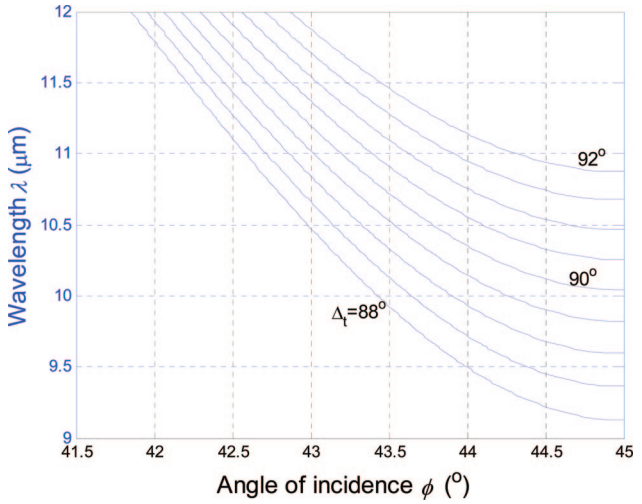

Fig. 9. (Color online) Wavelength λ in micrometers is plotted versus angle of incidence ϕ in degrees such that the cumulative retardance $\Delta_t(\lambda, \phi)$ of a ZnS-coated Si right-angle prism assumes constant values from 88° to 92° in steps of 0.5°.

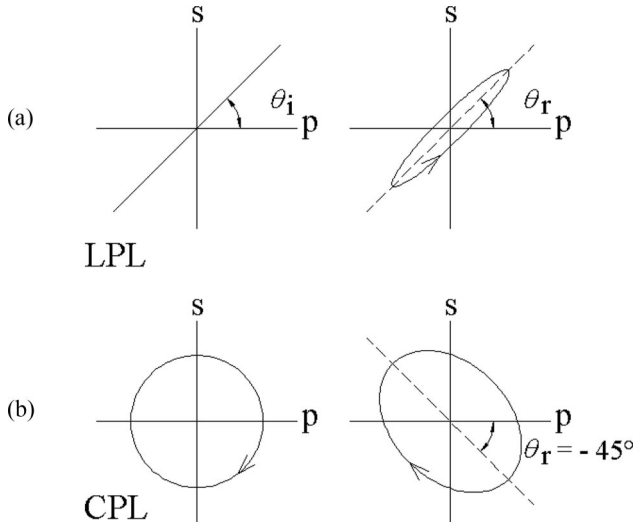

Fig. 10. Transformation of incident (a) linearly and (b) circularly polarized light upon retroreflection by a high-index (PbTe) right-angle prism.

The maximum extinction ratio is $e^2 = b^2/a^2 = 8.17 \times 10^{-4}$ for $n = 6$ and $\theta_i = 45°$, so that the reflected light is essentially LP.

For incident right-handed circularly polarized (RHCP) light, the reflected light is also nearly RHCP [Fig. 10(b)]. [The reflected polarization is closer to circular than is shown in Fig. 10(b).] The major-axis azimuth θ_r and ellipticity angle ε_r of the reflected near-circular state are given by

$$\theta_r = -45°, \qquad \varepsilon_r = 45° - (RE/2)°. \tag{15}$$

The polarization properties described above are readily verified by use of the Poincaré sphere or Mueller calculus [17]. Given the flat angular response $\Delta_t(\phi)$ for $n = 6$ in Fig. 3 and the strong ray bending at the air–PbTe interface (in accordance with Snell's law), the external (in-air) field of view of this device is limited only by the angular response of the antireflection coating at the entrance face of the prism.

6. In-Line Half-Wave Retarders

Exact HWR and in-line operation is achieved using the chevron dual-Fresnel rhomb of Fig. 11 with four TIRs at the same angle $\phi = 45°$. This compact design, which was first introduced in [4], has the most favorable (smallest) length/aperture aspect ratio of 2, as compared to longer in-line devices [3,5] that operate at higher angles of incidence. The cumulative retardance is double that given by Eqs. (1) and (4). For paraxial rays the first and second reflections occur at the same angle ϕ and the third and fourth reflections occur at the complementary angle $90° - \phi$. Therefore the analysis of Section 2 applies entirely to the in-line (and rotatable) HWR shown in Fig. 11 whose net retardance $\Delta_t(\phi)$ is also insensitive to angle-of-incidence errors. N-BAK4 Schott glass and ZnS-coated Si (as described in Sections 3 and 4) are excellent candidates for this in-line HWR design.

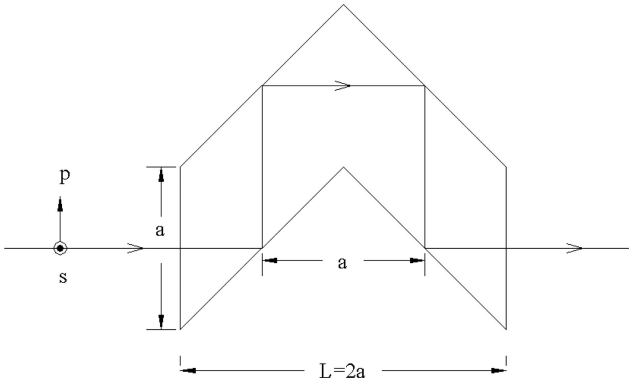

Fig. 11. In-line half-wave retarder using a chevron, dual-Fresnel-rhomb, prism with four TIR at the same angle of incidence $\phi = 45°$.

7. Summary

The cumulative phase retardance associated with total internal retroreflection by a right-angle prism is investigated. QWR is achieved with minimum angular sensitivity by a prism of refractive index $n = (\sqrt{2} + 1)^{1/2}$ in the symmetric orientation. Excellent performance (small retardance error) is obtained over two octaves in the visible and near-IR spectrum by use of an uncoated right-angle prism of N-BAK4 Schott glass. A Si prism, which has a noninterference coating of ZnS, is proposed for linear-to-circular polarization conversion of CO_2 laser radiation over a 2 μm bandwidth. A high-index ($n = 6$) PbTe right-angle prism acts as a near-HWR with maximally flat net retardance versus angle of incidence. However, because of retroreflection, this interesting device nearly preserves the state of polarization of light, for all input states, and over a large field of view. Finally, a useful algorithm is given in Appendix A that transforms a three-term Sellmeier dispersion relation of a transparent optical material to an equivalent cubic equation that can be solved for the wavelengths at which the refractive index assumes any desired value.

Appendix A

Substitution of

$$\eta = n^2 - 1, \qquad x = \lambda^2, \tag{A1}$$

in Eq. (11) leads to a cubic equation in x,

$$a_3 x^3 + a_2 x^2 + a_1 x + a_0 = 0, \tag{A2}$$

with coefficients given by

$$a_3 = S_B - \eta, \quad a_2 = (\eta - S_B)S_C + S_{BC},$$
$$a_1 = P_C(S_{B/C} - \eta S_{1/C}), \quad a_0 = \eta P_C. \tag{A3}$$

In Eqs. (A3) the sums and products S and P are defined by

$$S_B = \sum_{i=1}^{3} B_i, \quad S_C = \sum_{i=1}^{3} C_i,$$

$$S_{1/C} = \sum_{i=1}^{3} (1/C_i), \quad S_{BC} = \sum_{i=1}^{3} (B_i C_i),$$

$$S_{B/C} = \sum_{i=1}^{3} (B_i/C_i), \quad P_C = C_1 C_2 C_3. \tag{A4}$$

Exact closed-form solutions of cubic equations are available [18].

References

1. M. Born and E. Wolf, *Principles of Optics* (Cambridge, 1999).
2. R. J. King, "Quarter-wave retardation systems based on the Fresnel rhomb principle," J. Sci. Instrum. **43,** 617–622 (1966).
3. J. M. Bennett, "Critical evaluation of rhomb-type quarterwave retarders," Appl. Opt. **9,** 2123–2129 (1970).
4. I. Filinski and T. Skettrup, "Achromatic phase retarders constructed from right-angle prisms: design," Appl. Opt. **23,** 2747–2751 (1984).
5. K. B. Rochford, P. A. Williams, A. H. Rose, I. G. Clarke, P. D. Hale, and G. W. Day, "Standard polarization components: progress toward an optical retardance standard," Proc. SPIE **2265,** 2–8 (1994).
6. N. N. Nagib and M. S. El-Bahrawy, "Phase retarders with variable angles of total internal reflection," Appl. Opt. **33,** 1218–1222 (1994).
7. A. M. Kan'an and R. M. A. Azzam, "In-line quarter-wave retarders for the IR using total refraction and total internal reflection in a prism," Opt. Eng. **33,** 2029–2033 (1994).
8. R. M. A. Azzam and M. M. K. Howlader, "Silicon-based polarization optics for the 1.30 and 1.55 μm communication wavelengths," J. Lightwave Technol. **14,** 873–878 (1996).
9. R. M. A. Azzam and C. L. Spinu, "Achromatic angle-insensitive infrared quarter-wave retarder based on total internal reflection at the Si-SiO_2 interface," J. Opt. Soc. Am. A **21,** 2019–2022 (2004).
10. R. M. A. Azzam and N. M. Bashara, *Ellipsometry and Polarized Light* (North-Holland, 1987), p. 253.
11. R. M. A. Azzam, "Measurement of the Jones matrix of an optical system by return-path null ellipsometry," Opt. Acta **28,** 795–800 (1981).
12. M. Shribak, "Polarimetric optical fiber refractometer," Appl. Opt. **40,** 2670–2674 (2001).
13. R. M. A. Azzam, "Phase shifts that accompany total internal reflection at a dielectric-dielectric interface," J. Opt. Soc. Am. A **21,** 1559–1563 (2004).
14. Data available at http://www.us.schott.com/optics_devices/english/products/flash/abbediagramm_flash.html.
15. W. J. Tropf, M. E. Thomas, and T. J. Harris, "Properties of crystals and glasses," in *Handbook of Optics,* M. Bass, E. W. Van Stryland, D. R. Williams, and W. L. Wolfe, eds. (McGraw-Hill, 1995), Vol. II.
16. R. M. A. Azzam and M. M. Howlader, "Fourth- and sixth-order polarization aberrations of antireflection-coated optical surfaces," Opt. Lett. **26,** 1607–1608 (2001).
17. R. M. A. Azzam and N. M. Bashara, *Ellipsometry and Polarized Light* (North-Holland, 1987), Chap. 2.
18. See, for example, J. J. Tuma, *Engineering Mathematics Handbook* (McGraw-Hill, 1987), p. 7.